Soft Computing
https://doi.org/10.1007/s00500-023-08315-5

APPLICATION OF SOFT COMPUTING

An efficient computational procedure to solve the biological nonlinear Leptospirosis model using the genetic algorithms

Zulqurnain Sabir[1,6] · Mohamed R. Ali[2,3] · Muhammad Asif Zahoor Raja[4] · R. Sadat[5]

Accepted: 22 April 2023

Abstract
The purpose of this work is to present the numerical solutions of the nonlinear mathematical Leptospirosis disease (LD) model using the computational performances of the artificial neural networks (ANNs) along with the optimization procedures based on the global search genetic algorithm (GA) and local search active-set algorithm (ASA) scheme, i.e., ANNs-GA-ASA. LD is a zoonotic disease that is occurring in the whole world, obtained by rodents that become the reason of death in the people. The LD model based on the susceptible-infected-recovered, i.e., SIR, is used to solve the mechanisms of disease spread. The optimization of an error-based fitness function, which is constructed through the differential mathematical system using the hybrid computing proficiencies of the ANNs-GA-ASA for solving the LD model. The stochastic ANNs-GA-ASA procedures are applied to the LD model to authenticate the precision, exactness, reliability and competence of the ANNs-GA-ASA. The obtained results using the ANNs-GA-ASA of the LD model will be compared using the Runge–Kutta scheme, which authenticate the importance of the ANNs-GA-ASA. Furthermore, statistical analysis through different actions for the LD model approve the convergence and precision of the ANNs-GA-ASA.

Keywords Leptospirosis disease model · Nonlinear · Artificial neural networks · Active-set algorithm · Reference solutions · Statistical procedures

1 Introduction

In recent decades, mathematics is applied to understand the system of transmission of viruses worldwide (Keeling 2001). A number of diseases spread in the world, like as hantavirus, Leptospirosis disease (LD) and dengue. Few spreading diseases from one person to another are recognized as infectious disease, while those diseases, which are normally produced by environmental factors or genetic are recognized as noninfectious viruses (Keeling and Rohani 2011). LD is a bacterial, animal disease-producing infection and even demise in humans (Thayaparan et al. 2013). The spread of the Leptospira is due to the urine of host animal, which can be obtained into soil or water. The host animal that carries Leptospira is not damaged itself (Lim et al. 2011). The humans could adopt the diseases if they got some cuts on their skin that suffer with urine-dirtied food, soil or water (Bhalraj and Azmi 2019). The outbreaks of LD suddenly occur, when the individuals used the dirty water, like as floodwaters (Triampo et al. 2007). The transmission rate is very occasional from one to another individual (El-Shahed 2014). Generally, the bacteria sources are cattle, sheep, pigs, dogs, goats, horses, rats, raccoons and mice (Goh et al. 2019).

Mathematical systems are known as one of the fundamental tools in signifying the suitable strategies to

✉ Mohamed R. Ali
mohamed.reda@bhit.bu.edu.eg

1 Department of Mathematics and Statistics, Hazara University, Mansehra, Pakistan

2 Faculty of Engineering and Technology, Future University in Egypt, New Cairo 11835, Egypt

3 Basic Engineering Science Department, Benha Faculty of Engineering, Benha University, Banha, Egypt

4 Future Technology Research Center, National Yunlin University of Science and Technology, 123 University Road, Section 3, Douliou, Yunlin 64002, Taiwan, ROC

5 Department of Mathematics, Zagazig Faculty of Engineering, Zagazig University, Zagazig, Egypt

6 Department of Computer Science and Mathematics, Lebanese American University, Beirut, Lebanon

Published online: 14 June 2023

eliminate or minimize the LD and to predict the outbreaks of its future occurrences (Khan et al. 2021). Several differential equation-based models have been discussed by the researchers to designate the dynamical forms of both rat and human population. Kongnuy (Kongnuy 2012) proposed a mathematical system for the spreading of LD between vector population and the humans. It is observed that the control of LD is possible by lessening the rate of transmission of Leptospirosis from an infected to susceptible vector as well as human. Khan et al. (Khan et al. 2016) provided the dynamical performance of LD by considering the saturated occurrence rate that means the susceptible population reduced to follow the operative connection with the vectors and infected individuals. The simulation of the proposed system through the infection force rate is 0.83 that is used to lessen the LD transmission risk. Few other diseases that the world has been facing are provided in these references (Sánchez et al. 2020; Sabir et al. 2021a; Guerrero Sánchez et al. 2020; Umar et al. 2020a).

The purpose of this study is to present the numerical performances of the nonlinear LD mathematical model using an intelligent computational approach based on the artificial neural networks (ANNs) with the optimal performances of the global search genetic algorithm (GA) and local search active-set algorithm (ASA) schemes, i.e., ANNs-GA-ASA. The numerical stochastic procedures have been applied to solve various differential systems. However, the ANNs-GA-ASA procedures have never been executed to solve the LD nonlinear model. Recently, a few reported applications of the stochastic problem solver are functional systems (Sabir et al. 2020a; Guirao, et al. 2020), eye surgery system (Umar et al. 2019a), Thomas–Fermi type of model (Sabir et al. 2018), prey-predator form of the model (Umar et al. 2019b), HIV-based infection system (Umar et al. 2020b), periodic model (Sabir et al. 2020b), COVID-19 model (Sabir et al. 2021a), three-point system (Sabir 2020), multi-fractional systems (Sabir et al. 2020c), human head model (Raja et al. 2018) and mosquito dispersal model (Umar et al. 2020c). The current investigations are related to present the numerical formulations of the LD nonlinear model using the stochastic ANNs-GA-ASA procedures. The mathematical form of the LD nonlinear model is dependent upon three factors, susceptible-infected-recovered, i.e., SIR model. The SIR system has been applied to designate the Leptospirosis dynamic transmission. The SIR nonlinear system has both vector (rat) and human population. The mathematical form of the LD nonlinear system is presented as (Bhalraj et al. 2021) (Table 1):

$$\begin{cases} \frac{dS_h(\tau)}{d\tau} = A - \mu_h S_h(\tau) - \beta_h S_h(\tau) I_r(\tau) + \theta_h R_h(\tau), & S_h(0) = I_1, \\ \frac{dI_h(\tau)}{d\tau} = \beta_h S_h(\tau) I_r(\tau) - (\mu_h + \delta_h + r_h) I_h(\tau), & I_h(0) = I_2, \\ \frac{dR_h(\tau)}{d\tau} = r_h I_h(\tau) - (\mu_h + \theta_h) R_h(\tau), & R_h(0) = I_3, \\ \frac{dS_r(\tau)}{d\tau} = B - r_r S_r(\tau) - \beta_r S_r(\tau) I_h(\tau), & S_r(0) = I_4, \\ \frac{dI_r(\tau)}{d\tau} = \beta_r S_r(\tau) I_h(\tau) - (r_r + \delta_r) I_r(\tau), & I_r(0) = I_5, \end{cases} \tag{1}$$

Some important novelties of the proposed ANNs-GA-ASA for solving the LD system are provided as:

- A stochastic novel solver ANNs-GA-ASA is presented successfully for the numerical experimentations of the nonlinear biological LD nonlinear system.
- The log-sigmoid function is used as an activation/merit function for solving the mathematical LD system.
- The optimization of an error-based fitness function is presented using the hybrid computing framework GA-ASA.
- The correctness of the proposed ANNs-GA-ASA procedures are observed by comparing the obtained results and the reference solutions.
- The precision of the ANNs-GA-ASA is judged by finding the small AE for solving the mathematical LD system.
- For the stability of the proposed numerical ANNs-GA-ASA scheme, the statistical analysis in terms of variance account for (VAF), Theil's inequality coefficient (TIC) semi-interquartile (SIR) and mean absolute deviation (MAD) is provided.

The rest of the paper are summarized as: Section 2 narrates the methodology based on ANNs-GA-ASA and the mathematical forms of the statistical operators. Section 3 is provided based on the result's imitations. Section 4 is provided based on the concluding and future research remarks.

2 Designed methodology: ANNs-GA-ASA

In this section, the proposed ANNs-GA-ASA procedures are provided to solve the mathematical LD system. The methodology is drawn in two phases as:

- For the activation of the neural networks, an activation function using the ANNs-GA-ASA is provided.

- Necessary interpretations are provided to improve the fitness function using the hybrid computing GA-ASA framework.

2.1 Designed ANN procedure

The mathematical procedures of the LD nonlinear system are provided by designing the accomplished outcomes of the $\hat{S}_h(\tau)$, $\hat{I}_h(\tau)$, $\hat{R}_h(\tau)$, $S_r(\tau)$ and $I_r(\tau)$ along with the derivatives of each class, given as:

$$[\hat{S}_h(\tau),\ \hat{I}_h(\tau),\ \hat{R}_h(\tau), S_r(\tau), I_r(\tau)] = \begin{bmatrix} \sum_{i=1}^{m} q_{S_h,i} L(w_{S_h,i}\tau + v_{S_h,i}),\ \sum_{i=1}^{m} q_{I_h,i} L(w_{I_h,i}\tau + v_{I_h,i}), \\ \sum_{i=1}^{m} q_{R_h,i} L(w_{R_h,i}\tau + v_{R_h,i}), \sum_{i=1}^{m} q_{S_h,i} L(w_{S_r,i}\tau + v_{S_r,i}), \\ \sum_{i=1}^{m} q_{I_r,i} L(w_{I_r,i}\tau + v_{I_r,i}), \end{bmatrix}, \tag{2}$$

$$[\hat{S}_h^{(n)}(\tau),\ \hat{I}_h^{(n)}(\tau),\ \hat{R}_h^{(n)}(\tau), \hat{S}_r^{(n)}(\tau), \hat{I}_r^{(n)}(\tau)] = \begin{bmatrix} \sum_{i=1}^{m} q_{S_h,i} L^{(n)}(w_{S_h,i}\tau + v_{S_h,i}),\ \sum_{i=1}^{m} q_{I_h,i} L(w_{I_h,i}\tau + v_{I_h,i}), \\ \sum_{i=1}^{m} q_{R_h,i} L(w_{R_h,i}\tau + v_{R_h,i}), \sum_{i=1}^{m} q_{S_r,i} L(w_{S_r,i}\tau + v_{S_r,i}), \\ \sum_{i=1}^{m} q_{I_r,i} L(w_{I_r,i}\tau + v_{I_r,i}), \end{bmatrix},$$

The unidentified weights W are described as:

$W = [W_{S_h}, W_{I_h}, W_{R_h}, W_{S_h}, W_{I_h}]$, for $W_{S_h} = [q_{S_h}, \omega_{S_h}, v_{S_h}]$, $W_{S_h} = [q_{I_h}, \omega_{I_h}, v_{I_h}]$, $W_{R_h} = [q_{R_h}, \omega_{R_h}, v_{R_h}]$, $W_{S_h} = [q_{S_h}, \omega_{S_h}, v_{S_h}]$ and $W_{S_h} = [q_{I_h}, \omega_{I_h}, v_{I_h}]$, where

$$\begin{aligned}
q_{S_h} &= [q_{S_h,1}, q_{S_h,2}, ..., q_{S_h,m}], & q_{I_h} &= [q_{I_h,1}, q_{I_h,2}, ..., q_{I_h,m}], \\
q_{R_h} &= [q_{R_h,1}, q_{R_h,2}, ..., q_{R_h,m}], & & \\
q_{S_r} &= [q_{S_r,1}, q_{S_r,2}, ..., q_{S_r,m}], & q_{I_r} &= [q_{I_r,1}, q_{I_r,2}, ..., q_{I_r,m}], \\
w_{S_h} &= [w_{S_h,1}, w_{S_h,2}, ..., w_{S_h,m}], & & \\
w_{I_h} &= [w_{I_h,1}, w_{I_h,2}, ..., w_{I_h,m}], & w_{R_h} &= [w_{R_h,1}, w_{R_h,2}, ..., w_{R_h,m}], \\
w_{S_r} &= [w_{S_r,1}, w_{S_r,2}, ..., w_{S_r,m}], & & \\
w_{I_r} &= [w_{I_r,1}, w_{I_r,2}, ..., w_{I_r,m}], & v_{S_h} &= [v_{S_h,1}, v_{S_h,2}, ..., v_{S_h,m}], \\
v_{I_h} &= [v_{I_h,1}, v_{I_h,2}, ..., v_{I_h,m}], & & \\
v_{R_h} &= [v_{R_h,1}, v_{R_h,2}, ..., v_{R_h,m}], & v_{S_r} &= [v_{S_r,1}, v_{S_r,2}, ..., v_{S_r,m}], \\
v_{I_r} &= [v_{I_r,1}, v_{I_r,2}, ..., v_{I_r,m}]. & &
\end{aligned}$$

The log-sigmoid function as a neural network using the stochastic ANNs-GA-ASA procedures has never been implemented to solve the LD model, mathematically given as:

$L(\tau) = (1 + e^{-\tau})^{-1}$.

The updated form of system (2) is written as:

$$[\hat{S}_h(\tau), \hat{I}_h(\tau),\ \hat{R}_h(\tau), \hat{S}_r(\tau), \hat{I}_r(\tau)] = \begin{bmatrix} \sum_{i=1}^{m} \frac{q_{S_h,i}}{1+e^{-\left(w_{S_h,i}\tau + v_{S_h,i}\right)}},\ \sum_{i=1}^{m} \frac{q_{I_h,i}}{1+e^{-\left(w_{I_h,i}\tau + v_{I_h,i}\right)}}, \\ \sum_{i=1}^{m} \frac{q_{R_h,i}}{1+e^{-\left(w_{R_h,i}\tau + v_{R_h,i}\right)}}, \sum_{i=1}^{m} \frac{q_{S_r,i}}{1+e^{-\left(w_{S_r,i}\tau + v_{S_r,i}\right)}}, \\ \sum_{i=1}^{m} \frac{q_{I_r,i}}{1+e^{-\left(w_{I_r,i}\tau + v_{I_r,i}\right)}} \end{bmatrix},$$

$$[\hat{S}_h'(\tau), \hat{I}_h'(\tau),\ \hat{R}_h'(\tau), \hat{S}_r'(\tau), \hat{I}_r'(\tau)] = \begin{bmatrix} \sum_{i=1}^{m} \frac{q_{S_h,i} w_{S_h,i} e^{-\left(w_{S_h,i}\tau + v_{S_h,i}\right)}}{\left(1+e^{-\left(w_{S_h,i}\tau + v_{S_h,i}\right)}\right)^2},\ \sum_{i=1}^{m} \frac{q_{I_h,i} w_{I_h,i} e^{-\left(w_{I_h,i}\tau + v_{I_h,i}\right)}}{\left(1+e^{-\left(w_{I_h,i}\tau + v_{I_h,i}\right)}\right)^2}, \\ \sum_{i=1}^{m} \frac{q_{R_h,i} w_{R_h,i} e^{-\left(w_{R_h,i}\tau + v_{R_h,i}\right)}}{\left(1+e^{-\left(w_{R_h,i}\tau + v_{R_h,i}\right)}\right)^2}, \sum_{i=1}^{m} \frac{q_{S_r,i} w_{S_r,i} e^{-\left(w_{S_r,i}\tau + v_{S_r,i}\right)}}{\left(1+e^{-\left(w_{S_r,i}\tau + v_{S_r,i}\right)}\right)^2}, \\ \sum_{i=1}^{m} \frac{q_{I_r,i} w_{I_r,i} e^{-\left(w_{I_r,i}\tau + v_{I_r,i}\right)}}{\left(1+e^{-\left(w_{I_r,i}\tau + v_{I_r,i}\right)}\right)^2} \end{bmatrix}. \tag{3}$$

A merit function using the differential system is provided as:

$$e = \sum_{j=i}^{6} e_j \tag{4}$$

$$e_1 = \frac{1}{N}\sum_{i=1}^{N}\left[(\hat{S}_h')_i - A + \mu_h \hat{S}_h + \beta_h \hat{I}_r \hat{S}_h - \theta_h \hat{R}_h\right]^2, \tag{5}$$

$$e_2 = \frac{1}{N}\sum_{i=1}^{N}\left[(\hat{I}_h')_i - \beta_h I_r S_h + (\mu_h + \delta_h + r_h) I_h\right]^2, \tag{6}$$

$$e_3 = \frac{1}{N}\sum_{i=1}^{N}\left[(\hat{R}_h')_i - r_h \hat{I}_h + (\mu_h + \theta_h)\hat{R}_h\right]^2, \tag{7}$$

$$e_4 = \frac{1}{N}\sum_{i=1}^{N}\left[(\hat{S}_r')_i - \mathrm{B} + r_r \hat{S}_r + \beta_r \hat{S}_r \hat{I}_r\right]^2, \tag{8}$$

$$e_5 = \frac{1}{N}\sum_{i=1}^{N}\left[(\hat{I}_r')_i - \beta_r \hat{I}_r \hat{S}_h + (r_r + \delta_r) I_r\right]^2, \tag{9}$$

$$e_6 = \frac{1}{5}\Big[\left((\hat{S}_h)_0 - I_1\right)^2 + \left((\hat{I}_h)_0 - I_2\right)^2 + \left((\hat{R}_h)_0 - I_3\right)^2 + \left((\hat{S}_r)_0 - I_4\right)^2 + \left((\hat{I}_r)_0 - I_5\right)^2\Big], \tag{10}$$

where $\left(\hat{S}_h\right)_i = S_h(\tau_i)$, $\left(\hat{I}_h\right)_i = I_h(\tau_i)$, $\left(\hat{R}_h\right)_i = R_h(\tau_i)$, $\left(\hat{S}_r\right)_i = S_r(\tau_i)$, $\left(\hat{I}_r\right)_i = I_r(\tau_i)$, $Nh = 1$, and $\tau_i = ih$. $\hat{S}_i$, $\hat{I}_i$, $\hat{R}_i$, $\hat{S}_i$ and $\hat{I}_i$ represent the proposed outcomes of each class of the LD system. Whereas, e_1, e_2, e_3, e_4, e_5 and e_6 represent an error function associated with LD model (1). The error function e_6 is an error function based on the ICs.

Table 1 Comprehensive detail of each class and parameter of the LD system

Parameter	Descriptions
$S_h(\tau)$	Susceptible human
$I_h(\tau)$	Infected human
$R_h(\tau)$	Recovered human
$S_r(\tau)$	Susceptible rat
$I_r(\tau)$	Infected rat
A	Human population's recruitment rate
μ_h	Natural rate of death of human population
β_h	LD transmission rate from an infected to susceptible (rat to human)
θ_h	Immune individual's rate that again become susceptible
δ_h	Infected human's rate who dies through disease
r_h	Human's recovery rate
B	Rat population's recruitment rate
r_r	Rate of natural death of the population of rate
β_r	Rate of transmission through LD from infected to susceptible (rat to rat)
δ_r	Infected rate due to which rate dies
$I_1, I_2, ..., I_5$	ICs

2.2 Optimization procedure: GA-ASA

The optimization performances are presented to solve the LD mathematical model using the proposed ANN-GA-ASA. The proposed structure ANNs-GA-ASA to solve the LD model is presented in Fig. 1.

GA is an optimization-based process, which is used to solve the LD mathematical model using the proposed ANN-GA-ASA. It is performed for both unconstrained and constrained models by executing the selection of the best outcomes. It is realistic normally to control the precise population outcomes for several stiff or complex systems in terms of the optimal training. To accomplish the outcomes of the best model, GA work through the reproduction, mutation and crossover operators. Few contemporary GA's submissions are information and software technology (Oliveira et al. 2010), classic job-shop scheduling problems (SHl, G.U.O.Y.O.N.G. 1997), nuclear reactor core design optimization problem (Pereira and Lapa 2003), robotic manipulator (Ayala and Santos Coelho 2012), image denoising problem (Paiva et al. 2016), transonic wing optimization (Oyama et al. 2001), air-blast prediction (Armaghani et al. 2018), complex steel structures (Gero et al. 2005), microarray cancer classification (Motieghader et al. 2017), multi-level capacitated lot sizing problem with backlogging (Toledo et al. 2013), prediction liver disease system (Hassoon et al. 2017) and weapon–target assignment problems (Lee et al. 2003).

ASA is also a well-known local search optimization procedure that is broadly implemented in for both constrained and unconstrained systems. ASA has been applied to solve the various intricate and non-stiff models. Recently, ASA is implemented for real-time optimal control systems (Quirynen et al. 2018), pressure-dependent model of water distribution systems (Deuerlein et al. 2019), American lookback put option pricing (Song et al. 2017), non-smooth contact dynamics (Abide et al. 2021), nonlinear problems with monotone operators (He and Yang 2019) and multi-rigid-body dynamic contact problems (Barboteu and Dumont 2018). The GA-ASA hybridization procedure is used to control the sluggishness of the global GA operator. The ANNs-GA-ASA procedure is provided in Table 2.

2.3 Performance indices

In this section, the statistical performances based on the mathematical formulations are provided using the VAF, SIR, TIC and MAD together with the Global VAF, TIC and MAD to solve the LD system as:

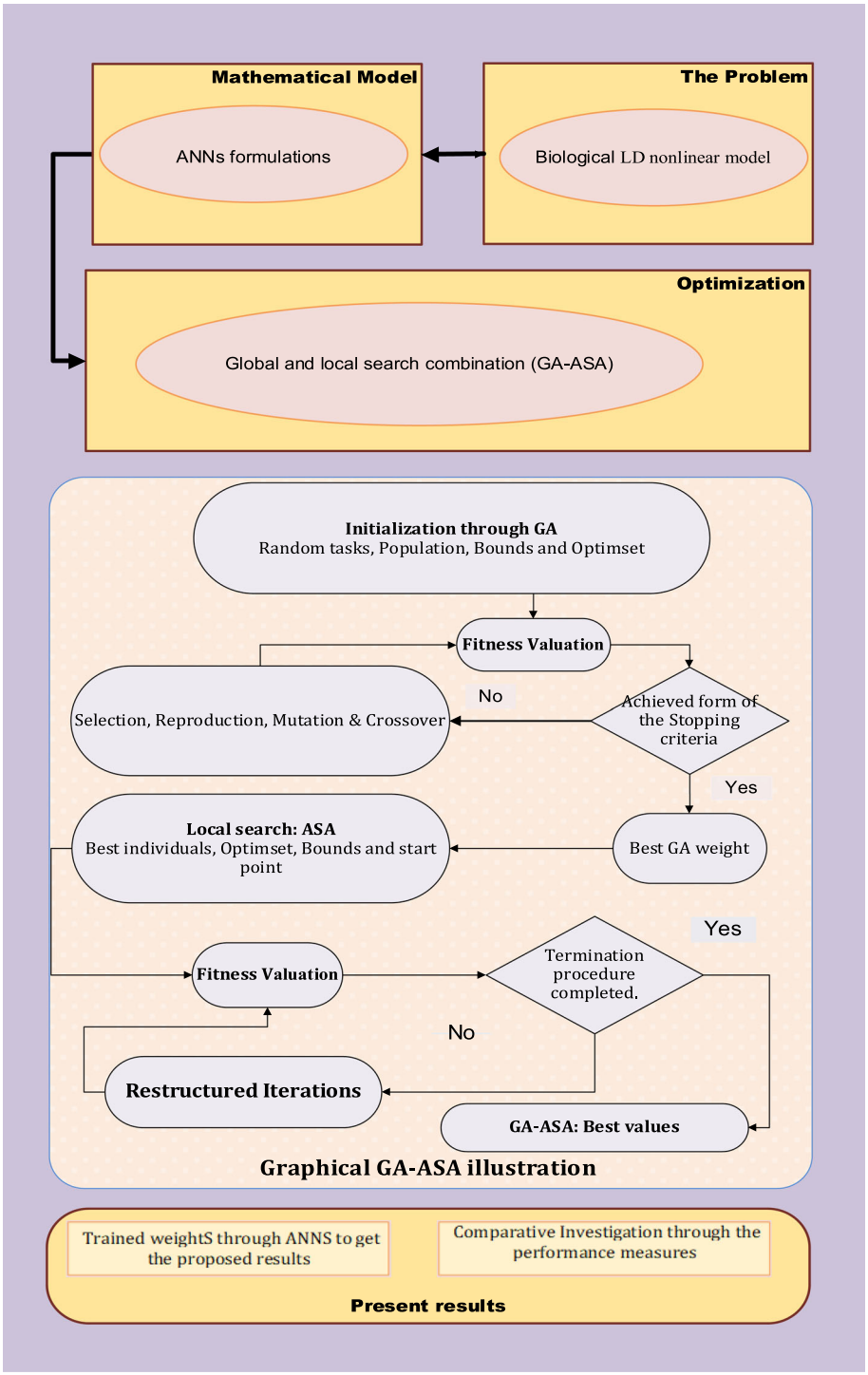

Fig. 1 Proposed structure through ANNs-GA-ASA to solve the LD model

$$\begin{cases} \begin{bmatrix} \mathrm{VAF}_{S_h}, & \mathrm{VAF}_{I_h}, \\ \mathrm{VAF}_{R_h}, & \mathrm{VAF}_{S_r}, \\ \mathrm{VAF}_{I_r} \end{bmatrix} = \begin{bmatrix} \left(1-\frac{\mathrm{var}\left((S_h)_r-\left(\hat{S_h}\right)_r\right)}{\mathrm{var}(S_h)}\right)*100, \left(1-\frac{\mathrm{var}\left((I_h)_r-\left(\hat{I_h}\right)_r\right)}{\mathrm{var}(I_h)}\right)*100, \\ \left(1-\frac{\mathrm{var}\left((R_h)_r-\left(\hat{R_h}\right)_r\right)}{\mathrm{var}(R_h)}\right)*100, \left(1-\frac{\mathrm{var}\left((S_r)_r-\left(\hat{S_r}\right)_r\right)}{\mathrm{var}(S_r)}\right)*100, \\ \left(1-\frac{\mathrm{var}\left((I_r)_r-\left(\hat{I_r}\right)_r\right)}{\mathrm{var}(I_r)}\right)*100, \end{bmatrix} \\ \begin{bmatrix} \mathrm{EVAF}_{S_h}, & \mathrm{EVAF}_{I_h}, \\ \mathrm{EVAF}_{R_h}, & \mathrm{EVAF}_{S_r}, \\ \mathrm{EVAF}_{I_r} \end{bmatrix} = \left[\begin{vmatrix} 100-\mathrm{VAF}_{S_h}, 100-\mathrm{VAF}_{I_h}, 100-\mathrm{VAF}_{R_h}, \\ 100-\mathrm{VAF}_{S_r}, 100-\mathrm{VAF}_{I_r} \end{vmatrix}\right]. \end{cases} \tag{11}$$

$$\begin{cases} \text{S.I Range} = -0.5\times(Q_1-Q_3), \\ Q_1 = \text{1st quartile } \& Q_1 = \text{3 rd quartile}, \end{cases} \tag{12}$$

$$\begin{bmatrix} \mathrm{TIC}_{S_h}, & \mathrm{TIC}_{I_h}, \\ \mathrm{TIC}_{R_h}, & \mathrm{TIC}_{S_r}, \\ \mathrm{TIC}_{I_r} \end{bmatrix} = \begin{bmatrix} \frac{\sqrt{\frac{1}{n}\sum_{r=1}^{n}\left((S_h)_r-\left(\hat{S_h}\right)_r\right)^2}}{\left(\sqrt{\frac{1}{n}\sum_{r=1}^{n}(S_h)_r^2}+\sqrt{\frac{1}{n}\sum_{r=1}^{n}\left(\hat{S_h}\right)_r^2}\right)}, \frac{\sqrt{\frac{1}{n}\sum_{r=1}^{n}\left((I_h)_r-\left(\hat{I_h}\right)_r\right)^2}}{\left(\sqrt{\frac{1}{n}\sum_{r=1}^{n}(I_h)_r^2}+\sqrt{\frac{1}{n}\sum_{r=1}^{n}\left(\hat{I_h}\right)_r^2}\right)}, \\ \frac{\sqrt{\frac{1}{n}\sum_{r=1}^{n}\left((R_h)_r-\left(\hat{R_h}\right)_r\right)^2}}{\left(\sqrt{\frac{1}{n}\sum_{r=1}^{n}(R_h)_r^2}+\sqrt{\frac{1}{n}\sum_{r=1}^{n}\left(\hat{R_h}\right)_r^2}\right)}, \frac{\sqrt{\frac{1}{n}\sum_{r=1}^{n}\left((S_r)_r-\left(\hat{S_r}\right)_r\right)^2}}{\left(\sqrt{\frac{1}{n}\sum_{r=1}^{n}(S_r)_r^2}+\sqrt{\frac{1}{n}\sum_{r=1}^{n}\left(\hat{S_r}\right)_r^2}\right)}, \\ \frac{\sqrt{\frac{1}{n}\sum_{r=1}^{n}\left((I_r)_r-\left(\hat{I_r}\right)_r\right)^2}}{\left(\sqrt{\frac{1}{n}\sum_{r=1}^{n}(I_r)_r^2}+\sqrt{\frac{1}{n}\sum_{r=1}^{n}\left(\hat{I_r}\right)_r^2}\right)} \end{bmatrix},$$

$$\left[\begin{bmatrix} \mathrm{MAD}_{S_h}, & \mathrm{MAD}_{I_h}, \\ \mathrm{MAD}_{R_h}, & \mathrm{MAD}_{S_r}, \\ \mathrm{MAD}_{I_r} \end{bmatrix}\right] = \left[\sum_{r=1}^{n}\left|S_r-\hat{S_r}\right|, \sum_{r=1}^{n}\left|I_r-\hat{I_r}\right|, \sum_{r=1}^{n}\left|R_r-\hat{R_r}\right|, \sum_{r=1}^{n}\left|S_r-\hat{S_r}\right|, \sum_{r=1}^{n}\left|I_r-\hat{I_r}\right|\right]$$

where the proposed solutions are $\hat{S_h}(\tau)$, $\hat{I_h}(\tau)$, $\hat{R_h}(\tau)$, $S_r(\tau)$ and $I_r(\tau)$.

3 Simulations of the results

In this section, the numerical solutions of the LD nonlinear model are presented using the ANNs-GA-ASA. The correctness of the designed ANNs-GA-ASA is observed by using the comparison procedures of the obtained outcomes and the reference solutions. In addition, statistical operators' performances are provided to check the reliability, precision and accurateness of the ANN-GA-ASA. The simplified procedures based on the LD nonlinear model are presented using the suitable values, given as:

Table 2 Optimization performances through the ANN-GA-ASA for solving the nonlinear LD model

Start of process GA

Inputs: For the same number of system elements, the chromosome are given as:

$\boldsymbol{W} = [q, w, v]$

Population: The set of chromosomes are given as:

$\boldsymbol{W}_{S_h} = [\boldsymbol{q}_{S_h}, \boldsymbol{\omega}_{S_h}, \boldsymbol{v}_{S_h}]$, $\boldsymbol{W}_{S_h} = [\boldsymbol{q}_{I_h}, \boldsymbol{\omega}_{I_h}, \boldsymbol{v}_{I_h}]$, $\boldsymbol{W}_{R_h} = [\boldsymbol{q}_{R_h}, \boldsymbol{\omega}_{R_h}, \boldsymbol{v}_{R_h}]$, $\boldsymbol{W}_{S_h} = [\boldsymbol{q}_{S_h}, \boldsymbol{\omega}_{S_h}, \boldsymbol{v}_{S_h}]$ and $\boldsymbol{W}_{S_h} = [\boldsymbol{q}_{I_h}, \boldsymbol{\omega}_{I_h}, \boldsymbol{v}_{I_h}]$.

Output: The global values are identified as: $\boldsymbol{W}_{\text{Best-GA}}$

Initialization: To select the chromosomes, use the values of the weight vectors.

Fit Assessment: Compute the Fitness (e) in the population "***P***" for each vector using Eqs 4-8.

- **Stopping standards:** Stop if [PopSize=300], [$e = 10^{-10}$], [TolCon = 10^{-20}], [Generations = 65], [StallLimit=160] and [TolFun = 10^{-21}].

Move to [**storage]**

Ranking: Rank $\boldsymbol{W}$ in the population based on the fitness.

Storage: $\boldsymbol{W}_{\text{GA-Best}}$, time, e, iterations and function count in the GA presence.

End of [GA]

Process based ASA Starts

Inputs: $\boldsymbol{W}_{\text{Best-GA}}$

Output: $\boldsymbol{W}_{\text{GA-ASA}}$ represents the GA-ASA best values.

Initialize: $\boldsymbol{W}_{\text{Best-GA}}$, assignments, iterations and other standards.

Terminate: when [TolFun = 10^{-22}], [$e = 10^{-20}$], [TolX = 10^{-18}] [Iterations = 900], [MaxFunEvals= 267000], [TolCon= 10^{-22}] and accomplished.

Fitness Valuation: Calculate e and $\boldsymbol{W}$ for Eqs 4-8.

Amendments: Compute 'fmincon' for IPA, e of the best '**W**' values using Eqs 4-8

Accumulate: Transform $\boldsymbol{W}_{\text{GA-ASA}}$, function counts, e, time and iterations for the present ASA trials.

ASA process End

$$
\begin{cases}
\dfrac{\mathrm{d}S_h(\tau)}{\mathrm{d}\tau} = 1.6 - 0.03S_h(\tau) - 0.0098S_h(\tau)I_r(\tau) + 0.0067R_h(\tau), & S_h(0) = 100, \\
\dfrac{\mathrm{d}I_h(\tau)}{\mathrm{d}\tau} = 0.0098S_h(\tau)I_r(\tau) - (0.034 + 0.0001 + 0.007)I_h(\tau), & I_h(0) = 20, \\
\dfrac{\mathrm{d}R_h(\tau)}{\mathrm{d}\tau} = 0.007I_h(\tau) - (0.034 + 0.0067)R_h(\tau), & R_h(0) = 30, \\
\dfrac{\mathrm{d}S_r(\tau)}{\mathrm{d}\tau} = 1.2 - 0.17S_r(\tau) - 0.078S_r(\tau)I_h(\tau), & S_r(0) = 50, \\
\dfrac{\mathrm{d}I_r(\tau)}{\mathrm{d}\tau} = 0.078S_r(\tau)I_h(\tau) - (0.17 + 0.094)I_r(\tau), & I_r(0) = 10,
\end{cases}
$$

The fitness formulation of the above LD model is given as:

$$e = \frac{1}{N}\sum_{i=1}^{N}\begin{pmatrix} \left[\hat{S'}_h - 1.6 + 0.03\hat{S}_h + 0.0098\hat{I}_h\hat{S}_h - 0.0067\hat{R}_h\right]^2 \\ +\left[\hat{I'}_h - 0.0098\hat{I}_h\hat{S}_h + (0.034 + 0.0001 + 0.007)\hat{I}_h\right]^2 + \\ \left[\hat{R'}_h - 0.007\hat{I}_h + (0.034 + 0.0067)\hat{R}_h\right]^2 + \left[\hat{S'}_r - 1.2 + 0.17\hat{S}_r + 0.078\hat{S}_r\hat{I}_h\right]^2 \\ +\left[\hat{I'}_r - 0.078\hat{S}_r\hat{I}_h + (0.17 + 0.094)\hat{I}_r\right]^2 \end{pmatrix} + \frac{1}{5}\left[\left((\hat{S}_h)_0 - 100\right)^2 + \left((\hat{I}_h)_0 - 20\right)^2 + \left((\hat{R}_h)_0 - 30\right)^2 + \left((\hat{S}_r)_0 - 50\right)^2 + \left((\hat{I}_r)_0 - 10\right)^2\right]. \tag{15}$$

The optimization procedures of the mathematical form of the LD nonlinear model are provided in the system (1) using the designed ANNs-GA-ASA for 20 executions to attain the ANNs parameters for 30 variables. These best weights are graphically depicted in Fig. 2 using the ANNs-GA-ASA. The mathematical formulations of these results using the ANNs-GA-ASA is provided as:

$$\hat{S}_h(\tau) = \frac{10.1686}{1+e^{-(2.0340\tau+0.6797)}} + \frac{11.9962}{1+e^{-(1.6731\tau-4.2375)}} + \frac{13.2305}{1+e^{-(1.8647\tau-1.2468)}} + \frac{12.1410}{1+e^{-(0.4954\tau-3.0602)}} + \frac{4.3286}{1+e^{-(1.2739\tau-1.8647)}} + \frac{13.4688}{1+e^{-(1.5108\tau-4.8984)}} + \frac{9.6913}{1+e^{-(1.8335\tau-2.9083)}} - \frac{-13.6779}{1+e^{-(0.1682\tau+3.0333)}} + \frac{12.2248}{1+e^{-(0.3162\tau-2.6906)}} + \frac{12.1817}{1+e^{-(1.4416\tau-4.7405)}}. \tag{16}$$

$$\hat{I}_h(\tau) = \frac{6.7290}{1+e^{-(-1.5569\tau-0.8752)}} + \frac{6.8262}{1+e^{-(-0.9157\tau-2.6390)}} - \frac{-7.2885}{1+e^{-(-0.5934\tau-2.7455)}} - \frac{-2.4238}{1+e^{-(1.6872\tau-0.0115)}} - \frac{-0.1421}{1+e^{-(0.5881\tau-0.6073)}} - \frac{2.9045}{1+e^{-(2.7461\tau-0.7957)}} + \frac{3.6624}{1+e^{-(1.8993\tau-0.0145)}} - \frac{-6.9120}{1+e^{-(-37131\tau+5.3978)}} + \frac{0.8630}{1+e^{-(0.8739\tau+1.2310)}} + \frac{8.6236}{1+e^{-(2.6805\tau+2.4170)}}. \tag{17}$$

$$\hat{R}_h(\tau) = \frac{0.1870}{1+e^{-(0.0331\tau+1.1073)}} + \frac{1.9469}{1+e^{-(-0.1922\tau-0.7892)}} - \frac{-6.3381}{1+e^{-(-0.1922\tau-2.8190)}} - \frac{-6.2290}{1+e^{-(0.2588\tau-3.2529)}} - \frac{-1.5843}{1+e^{-(0.1525\tau+0.2963)}} - \frac{-6.0515}{1+e^{-(0.3731\tau-2.5257)}} + \frac{6.0218}{1+e^{-(0.0758\tau-3.0172)}} - \frac{-0.5033}{1+e^{-(0.2677\tau+0.9137)}} + \frac{3.5919}{1+e^{-(0.3902\tau-2.1176)}} + \frac{3.8798}{1+e^{-(0.7988\tau+0.7244)}}. \tag{18}$$

$$\hat{S}_r(\tau) = \frac{-5.7763}{1+e^{-(1.2518\tau+0.4323)}} - \frac{5.3724}{1+e^{-(-4.1692\tau-1.6297)}} - \frac{-9.2164}{1+e^{-(0.3742\tau-4.1343)}} - \frac{-9.1827}{1+e^{-(1.9694\tau-2.8361)}} - \frac{-5.4583}{1+e^{-(1.9653\tau-1.4994)}} - \frac{-9.8710}{1+e^{-(2.4354\tau-0.1670)}} + \frac{8.5590}{1+e^{-(0.5903\tau-5.5591)}} - \frac{-8.8976}{1+e^{-(1.6371\tau+3.5148)}} + \frac{3.7746}{1+e^{-(1.9491\tau-1.2605)}} + \frac{9.2084}{1+e^{-(0.3875\tau-4.4712)}}. \tag{19}$$

$$\hat{I}_r(\tau) = \frac{3.6258}{1+e^{-(-2.0238\tau+0.2796)}} - \frac{-5.6888}{1+e^{-(2.0098\tau-1.8839)}} - \frac{-0.3102}{1+e^{-(0.3551\tau+0.7290)}} - \frac{-0.9529}{1+e^{-(-0.3086\tau+0.8686)}} - \frac{2.4362}{1+e^{-(-0.3086\tau+2.8478)}} - \frac{-7.1395}{1+e^{-(1.4371\tau+2.5166)}} + \frac{-1.6253}{1+e^{-(0.5808\tau-2.7691)}} - \frac{-4.6970}{1+e^{-(-0.9260\tau-1.0526)}} + \frac{0.8356}{1+e^{-(0.0738\tau+1.4467)}} + \frac{3.4949}{1+e^{-(-1.8758\tau+1.5604)}}. \tag{20}$$

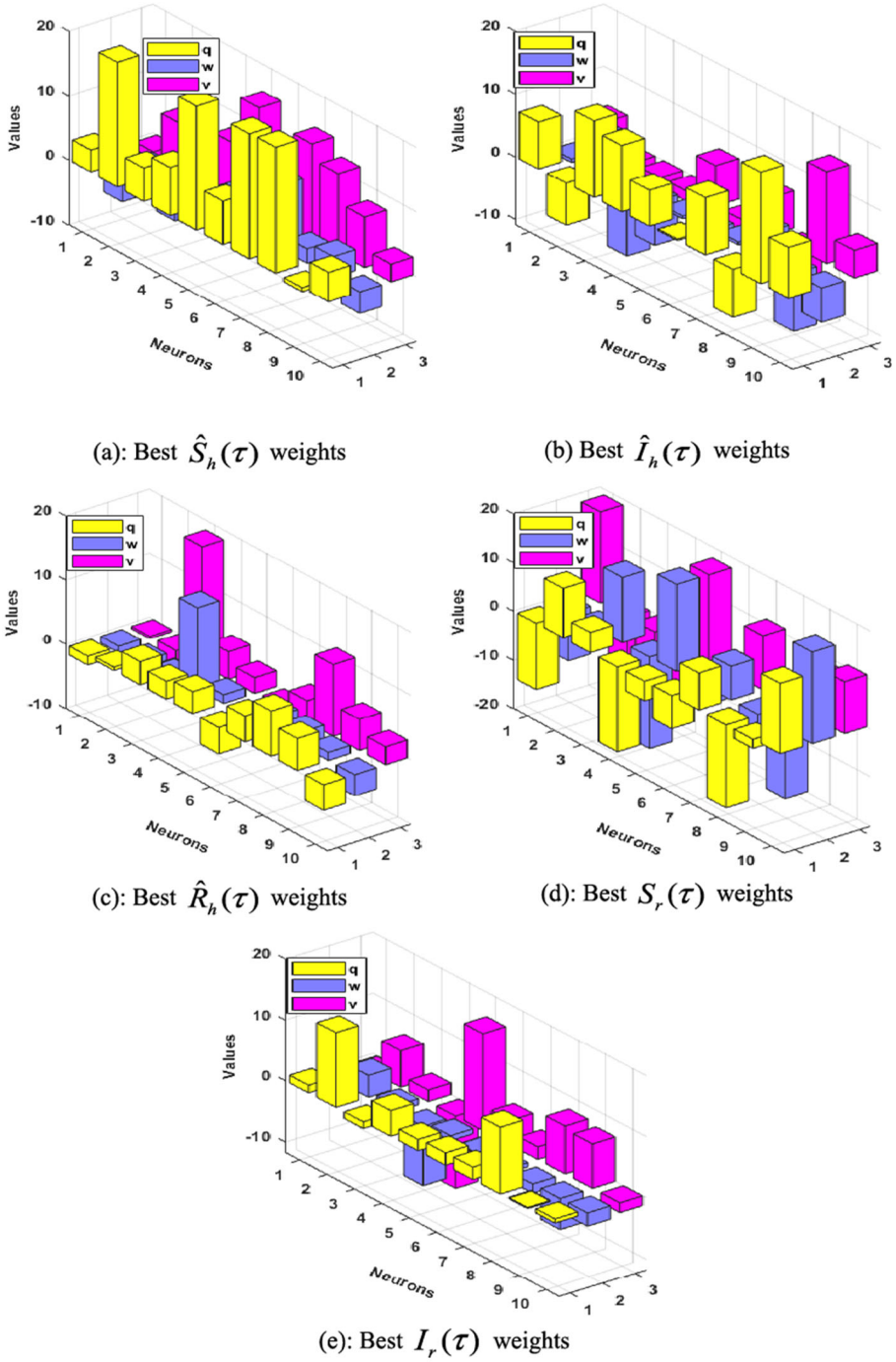

Fig. 2 Best weights of the ANNs-GA-ASA to solve the LD model

The above presented results of the LD nonlinear mathematical model using the stochastic ANNs-GA-ASA procedures are presented in Eqs. (16–20). The graphical representations of these results of the LD nonlinear mathematical model based on the best weights are provided in Fig. 2. The comparison of the best solutions obtained by the ANNs-GA-ASA for the LD model and the reference solutions is provided in Fig. 3. It is depicted that the best solutions obtained through the ANNs-GA-ASA are overlapped with the reference solutions, which indicate the correctness of the proposed numerical scheme. The AE values (Mean and Best) based on the LD nonlinear mathematical model are depicted in Fig. 4a–e for the classes $\hat{S}_h(\tau)$, $\hat{I}_h(\tau)$, $\hat{R}_h(\tau)$, $S_r(\tau)$ and $I_r(\tau)$, respectively. The 1st category of the LD model, i.e., $\hat{S}_h(\tau)$, which indicates the mean values have been calculated around 10^{-04}–10^{-05}, whereas the best AE is calculated around 10^{-05}–10^{-07}. The 2nd category of the LD model, i.e., $\hat{I}_h(\tau)$, that represents the

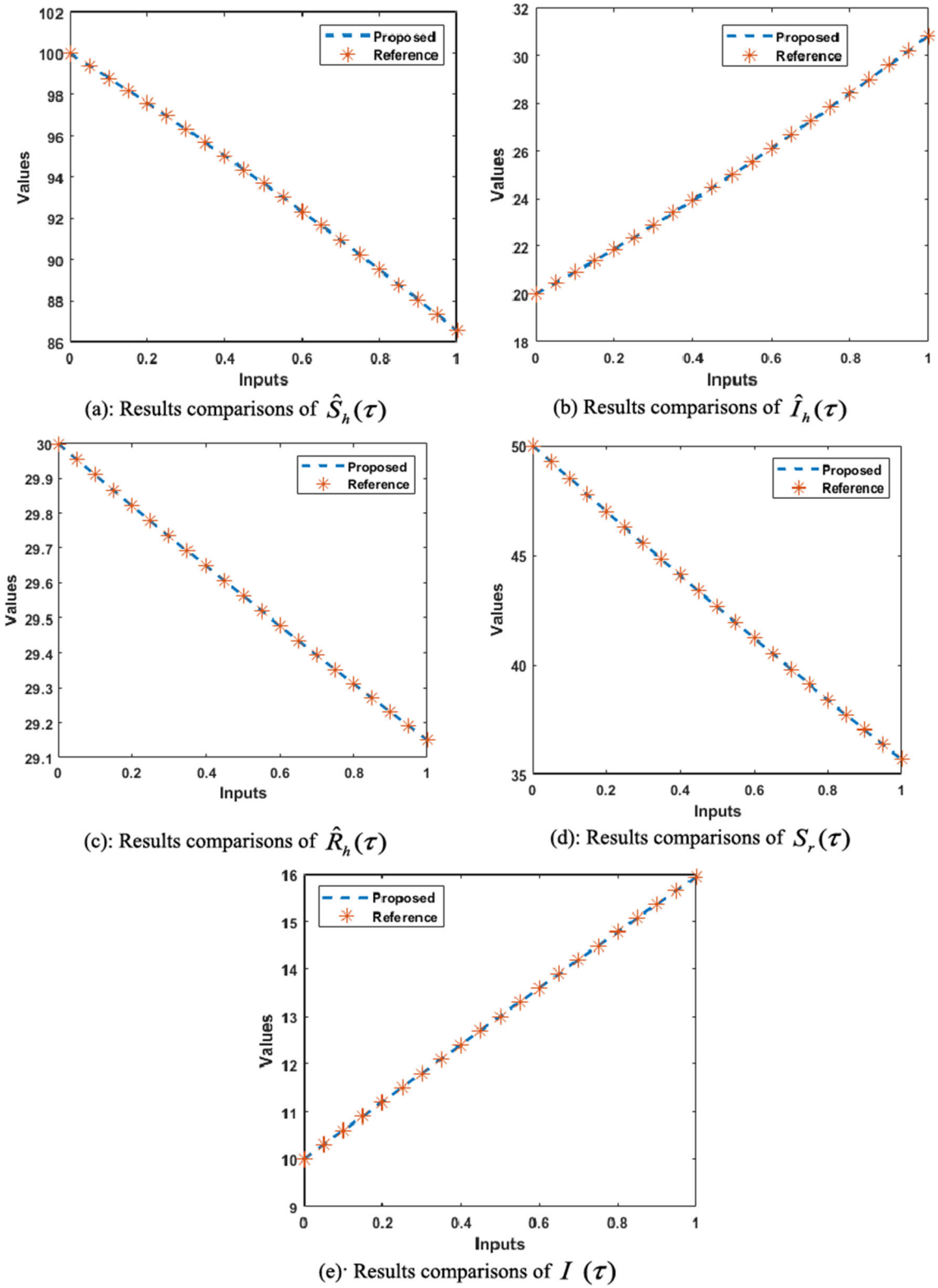

Fig. 3 Result comparisons of the ANNs-GA-ASA to solve the LD model

mean values have been calculated around 10^{-04}–10^{-05}, whereas the best AE is calculated around 10^{-04}–10^{-06}. The 3rd category of the LD model, i.e., $\hat{I}_h(\tau)$, that signifies the mean values have been calculated around 10^{-04}–10^{-05}, whereas the best AE is calculated around 10^{-05}–10^{-07}. The 4th category of the LD model, i.e., $S_r(\tau)$ that denotes the

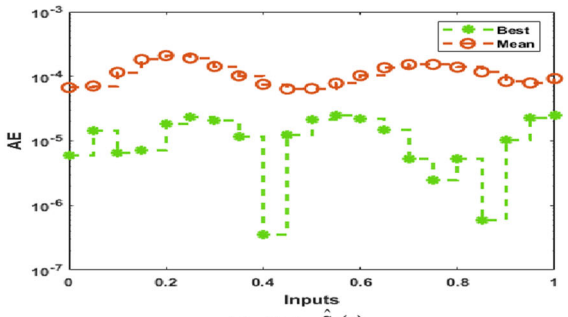

(a) AE for $\hat{S}_h(\tau)$

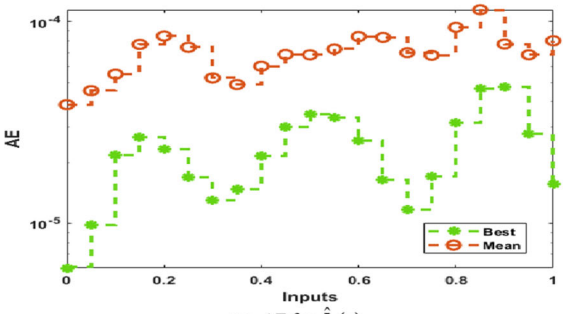

(b) AE for $\hat{I}_h(\tau)$

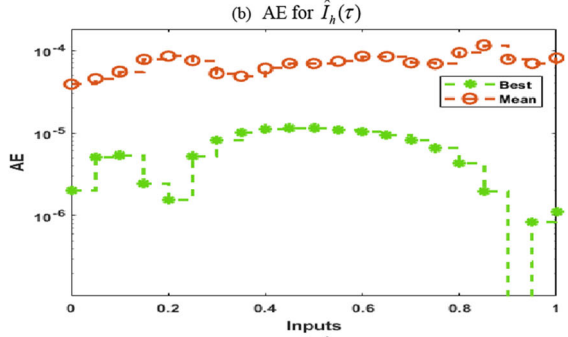

(c) AE for $\hat{R}_h(\tau)$

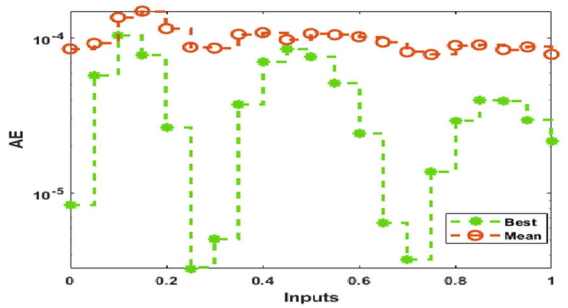

(d) AE for $S_r(\tau)$

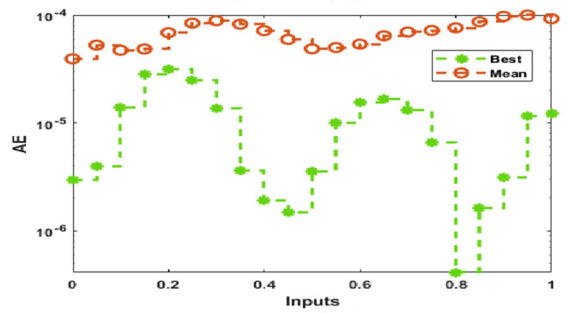

(e) AE for $I_r(\tau)$

◀**Fig. 4** AE values of the ANNs-GA-ASA to solve the LD model

mean values have been calculated around 10^{-03}–10^{-04}, whereas the best AE is calculated around 10^{-04}–10^{-06}. The 5th category of the LD model, i.e., $I_r(\tau)$ that symbolizes the mean values have been calculated around 10^{-04}–10^{-05}, whereas the best AE is calculated around 10^{-05}–10^{-07}. On these evidence based on the AE, one can observe that the designed ANNs-GA-ASA scheme is accurate for solving the LD nonlinear mathematical model. The performance is illustrated in Fig. 4 based on the EVAF, MAD and TIC operators for solving the LD nonlinear mathematical system using the proposed ANNs-GA-ASA. For the classes $\hat{S}_h(\tau)$, $\hat{I}_h(\tau)$, $\hat{R}_h(\tau)$, $S_r(\tau)$ and $I_r(\tau)$, the best EVAF, MAD and TIC operator values are calculated around 10^{-11}–10^{-12}, 10^{-05}–10^{-06} and 10^{-08}–10^{-10}, respectively.

The graphical depictions of the statistical EVAF, MAD and TIC procedures together with the histograms (HGs) are provided in Figures. 5, 6 and 7 for the classes $\hat{S}_h(\tau)$, $\hat{I}_h(\tau)$, $\hat{R}_h(\tau)$, $S_r(\tau)$ and $I_r(\tau)$ of the LD nonlinear mathematical model. The TIC, MAD and EVAF performances have calculated about 10^{-08}–10^{-10}, 10^{-09}–10^{-12} and 10^{-04}–10^{-06} for each category of the LD mathematical model. The obtained outcomes are performed satisfactorily using the ANNs-GA-ASA for solving the LD model.

To observe more accuracy and correctness, the statistical investigations using different statistical operators are explored in Tables 3, 4 and 5 for the LD nonlinear mathematical model. The statistical maximum (Max), minimum (Min), SIR, median (Med) and standard deviation (SD) operators have been provided in these investigations. The Min and Max operators observations indicate the best and bad performances in the 20 trials. For the classes $\hat{S}_h(\tau)$, $\hat{I}_h(\tau)$, $\hat{R}_h(\tau)$, $S_r(\tau)$ and $I_r(\tau)$, the Min, Max, Med, SIR and SD performances are calculated 10^{-06}–10^{-07}, 10^{-04}–

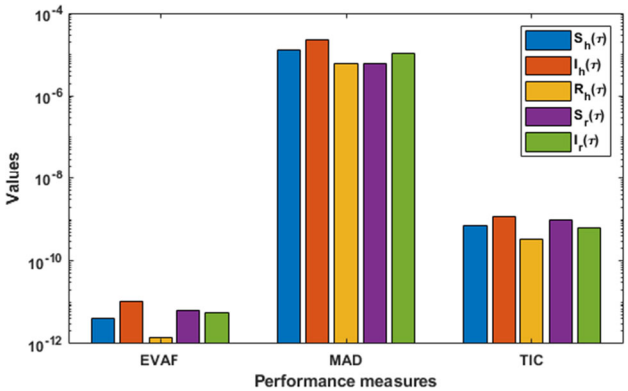

Fig. 5 Performance investigations of the EVAF, TIC and MAD statistical operators for solving the LD nonlinear mathematical model

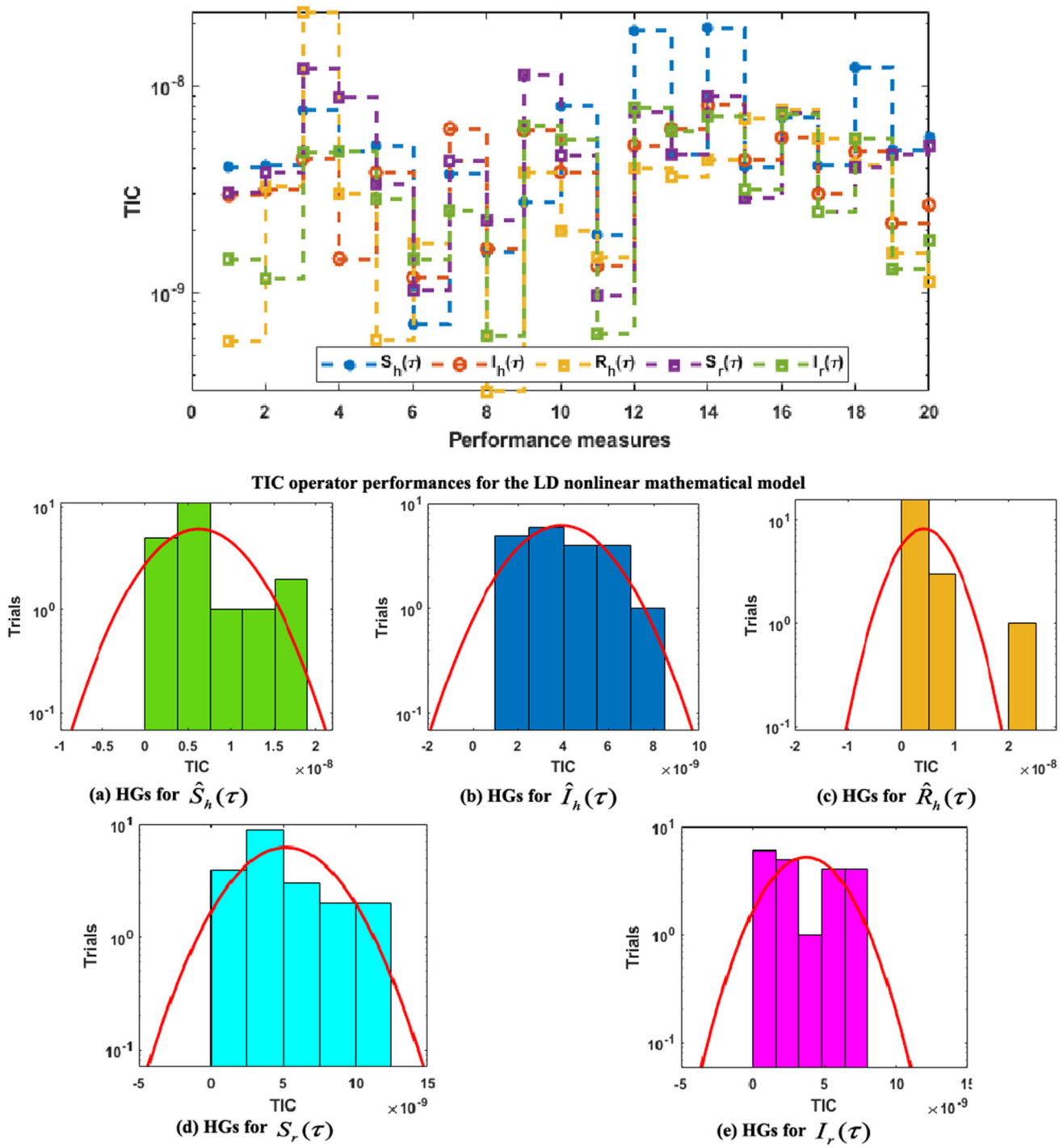

Fig. 6 TIC convergence plots along with HGs using ANNs-GA-ASA to solve the LP model

10^{-05}, 10^{-04}–10^{-06}, 10^{-05}–10^{-06} and 10^{-04}–10^{-05}, respectively. It is assumed to these performances that achieved results are precise and the stochastic ANNs-GA-ASA approach is accurate and stable (Table 6).

The global [G.MAD], [G.TIC] and [G.EVAF] operator's performances for 20 runs are provided using the ANNs-GA-ASA in Table 7 for the classes $\hat{S}_h(\tau)$, $\hat{I}_h(\tau)$, $\hat{R}_h(\tau)$, $S_r(\tau)$ and $I_r(\tau)$ of the LD model. The mean operator values are calculated 10^{-05}–10^{-06} for G.MAD, 10^{-09}–10^{-10} for G.TIC and 10^{-10}–10^{-11} for G.EVAF, whereas the SIR operator values are calculated 10^{-05}–10^{-06} for G.MAD, 10^{-08}–10^{-10} for G.TIC and 10^{-10}–10^{-12} for G.EVAF.

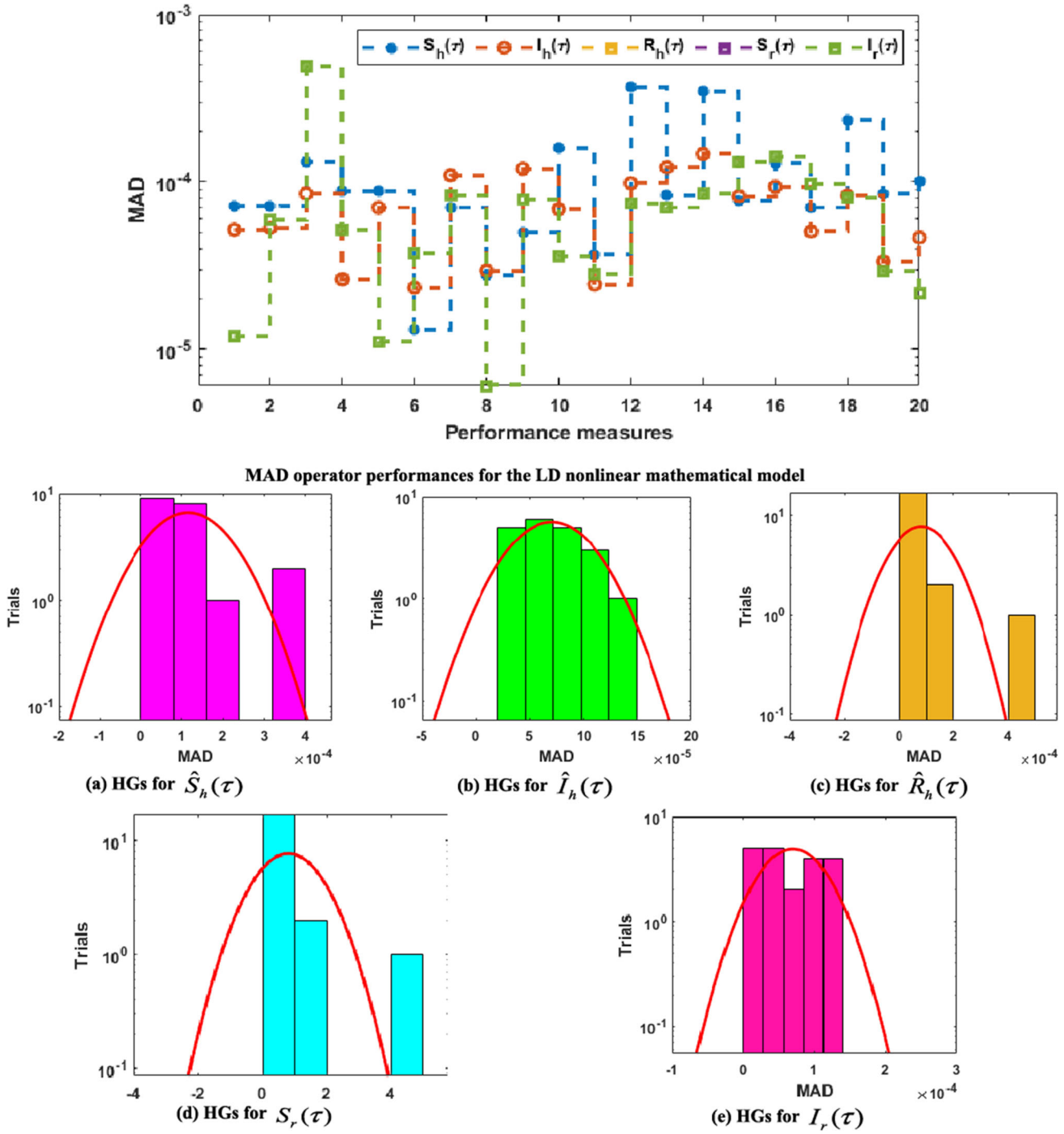

Fig. 7 MAD convergence plots along with HGs using ANNs-GA-ASA to solve the LP model

These optimal outcomes attained by the global operators approve the correctness, precision and accurateness of the designed ANNs-GA-ASA (Table 8) (Fig. 8).

4 Concluding remarks

The numerical investigations for solving the mathematical nonlinear Leptospirosis disease model have been presented in this study using the computational performances of the artificial neural networks along with the optimization

Table 3 Statistical form of the LD model for $\hat{S_h}(\tau)$ class

τ	$\hat{S_h}(\tau)$					
	Min	Max	Med	SIR	SD	Mean
0	4.06310E−06	4.01732E−04	2.12321E−05	3.76903E−05	9.65536E−05	2.12321E−05
0.05	9.22264E−07	5.18593E−04	3.12636E−05	3.76482E−05	1.16208E−04	3.12636E−05
0.1	6.45724E−06	7.01473E−04	7.18965E−05	4.68273E−05	1.54195E−04	7.18965E−05
0.15	7.11474E−06	7.17788E−04	1.43663E−04	6.65770E−05	1.59364E−04	1.43663E−04
0.2	1.80423E−05	5.67533E−04	1.77858E−04	6.71981E−05	1.53561E−04	1.77858E−04
0.25	1.24863E−05	6.13250E−04	1.62941E−04	7.29505E−05	1.49982E−04	1.62941E−04
0.3	4.69050E−06	5.62045E−04	1.07441E−04	7.03797E−05	1.46404E−04	1.07441E−04
0.35	1.11453E−05	4.45578E−04	6.54967E−05	4.08171E−05	1.18432E−04	6.54967E−05
0.4	3.55626E−07	3.09696E−04	4.34515E−05	4.33794E−05	8.53025E−05	4.34515E−05
0.45	1.36843E−06	2.00113E−04	3.76201E−05	4.41239E−05	5.76738E−05	3.76201E−05
0.5	1.77027E−07	2.35911E−04	5.47689E−05	3.48784E−05	5.78635E−05	5.47689E−05
0.55	5.90508E−06	3.79484E−04	4.55507E−05	2.96527E−05	8.97634E−05	4.55507E−05
0.6	5.66606E−07	5.01952E−04	6.07214E−05	4.97464E−05	1.23759E−04	6.07214E−05
0.65	1.47019E−05	5.77703E−04	8.83824E−05	4.68267E−05	1.40124E−04	8.83824E−05
0.7	5.21820E−06	5.91936E−04	1.21100E−04	5.03617E−05	1.54764E−04	1.21100E−04
0.75	2.44356E−06	6.00751E−04	1.19904E−04	6.27221E−05	1.63697E−04	1.19904E−04
0.8	3.39084E−06	5.99940E−04	8.47419E−05	7.26080E−05	1.61428E−04	8.47419E−05
0.85	5.95549E−07	5.10746E−04	6.52905E−05	5.47979E−05	1.33118E−04	6.52905E−05
0.9	5.35046E−06	3.65090E−04	5.07673E−05	3.27990E−05	9.60462E−05	5.07673E−05
0.95	5.00149E−06	2.45420E−04	4.50961E−05	5.56819E−05	7.20198E−05	4.50961E−05
1	6.24542E−07	2.94696E−04	6.78011E−05	6.54462E−05	8.17574E−05	6.78011E−05

Table 4 Statistical form of the LD model for $\hat{I_h}(\tau)$ class

τ	$\hat{I_h}(\tau)$					
	Min	Max	Med	SIR	SD	Mean
0	3.81731E−07	2.74265E−04	1.14969E−05	2.13478E−05	6.59161E−05	1.14969E−05
0.05	1.78736E−06	2.77378E−04	1.49237E−05	2.00138E−05	6.89380E−05	1.49237E−05
0.1	1.82424E−06	1.89645E−04	4.69822E−05	2.89818E−05	4.95933E−05	4.69822E−05
0.15	3.41471E−06	2.10768E−04	6.00441E−05	3.65090E−05	5.65419E−05	6.00441E−05
0.2	7.51298E−06	2.74575E−04	7.69521E−05	4.31945E−05	6.43410E−05	7.69521E−05
0.25	1.69347E−05	2.52064E−04	6.14568E−05	3.55237E−05	5.50185E−05	6.14568E−05
0.3	6.16607E−07	1.63134E−04	3.43155E−05	3.77156E−05	4.76352E−05	3.43155E−05
0.35	6.34889E−07	1.60060E−04	2.99499E−05	3.17396E−05	4.76143E−05	2.99499E−05
0.4	4.13034E−06	1.86694E−04	4.25204E−05	3.54425E−05	5.46824E−05	4.25204E−05
0.45	1.07185E−05	1.77100E−04	5.38296E−05	4.16040E−05	5.53310E−05	5.38296E−05
0.5	6.13482E−06	1.76253E−04	5.13575E−05	5.29214E−05	5.48253E−05	5.13575E−05
0.55	4.14047E−06	1.77602E−04	5.33223E−05	3.75160E−05	5.61608E−05	5.33223E−05
0.6	5.37483E−06	1.98252E−04	6.55977E−05	5.44345E−05	6.00627E−05	6.55977E−05
0.65	4.40234E−06	1.99919E−04	7.85660E−05	4.85259E−05	6.36211E−05	7.85660E−05
0.7	6.50345E−06	2.08730E−04	6.42744E−05	4.20236E−05	5.60099E−05	6.42744E−05
0.75	1.64844E−07	1.97627E−04	5.15039E−05	4.98413E−05	6.01582E−05	5.15039E−05
0.8	3.82317E−07	3.49505E−04	5.79019E−05	4.80465E−05	9.09718E−05	5.79019E−05
0.85	5.33774E−06	3.76612E−04	9.58554E−05	4.79818E−05	9.61864E−05	9.58554E−05
0.9	7.53997E−06	2.25004E−04	5.84311E−05	4.08060E−05	6.69978E−05	5.84311E−05
0.95	9.91500E−06	1.75512E−04	6.48132E−05	3.26522E−05	4.30635E−05	6.48132E−05
1	5.37780E−06	2.28713E−04	7.88743E−05	5.19625E−05	5.95776E−05	7.88743E−05

Table 5 Statistical form of the LD model for $\hat{R_h}(\tau)$ class

τ	$\hat{R_h}(\tau)$					
	Min	Max	Med	SIR	SD	Mean
0	1.77708E−06	4.39672E−04	2.34886E−05	2.88143E−05	9.65650E−05	2.34886E−05
0.05	1.93953E−06	3.67547E−04	6.03042E−05	3.24030E−05	8.03613E−05	6.03042E−05
0.1	3.74362E−06	3.37427E−04	6.03877E−05	3.93427E−05	7.60739E−05	6.03877E−05
0.15	2.45854E−06	3.39007E−04	5.31632E−05	2.80493E−05	7.44800E−05	5.31632E−05
0.2	3.72788E−07	3.63038E−04	2.56294E−05	2.41075E−05	7.97873E−05	2.56294E−05
0.25	5.26170E−06	4.01356E−04	3.32053E−05	1.26884E−05	8.74355E−05	3.32053E−05
0.3	3.04138E−07	4.46881E−04	4.70145E−05	3.24720E−05	9.93224E−05	4.70145E−05
0.35	6.05033E−06	4.93637E−04	4.50459E−05	4.10205E−05	1.11869E−04	4.50459E−05
0.4	8.38727E−06	5.36750E−04	6.08755E−05	4.78408E−05	1.23141E−04	6.08755E−05
0.45	6.68179E−06	5.72445E−04	6.20293E−05	4.70953E−05	1.31624E−04	6.20293E−05
0.5	5.66826E−06	5.98054E−04	6.97647E−05	4.56176E−05	1.37586E−04	6.97647E−05
0.55	5.46989E−06	6.12004E−04	6.82787E−05	4.51602E−05	1.40502E−04	6.82787E−05
0.6	6.09028E−06	6.13804E−04	5.20224E−05	4.46876E−05	1.40681E−04	5.20224E−05
0.65	1.60060E−06	6.04062E−04	2.65002E−05	3.99405E−05	1.39158E−04	2.65002E−05
0.7	4.05852E−06	5.84431E−04	2.83413E−05	2.88853E−05	1.31039E−04	2.83413E−05
0.75	6.44994E−06	5.57634E−04	3.52413E−05	3.23011E−05	1.21148E−04	3.52413E−05
0.8	4.29611E−06	5.27415E−04	4.55033E−05	3.46131E−05	1.13353E−04	4.55033E−05
0.85	1.95258E−06	4.98548E−04	5.29599E−05	4.04791E−05	1.07628E−04	5.29599E−05
0.9	6.80601E−08	4.76782E−04	5.42265E−05	5.14147E−05	1.04327E−04	5.42265E−05
0.95	8.27344E−07	4.68858E−04	5.13869E−05	3.64002E−05	1.01968E−04	5.13869E−05
1	6.86328E−07	4.82447E−04	2.57702E−05	4.19902E−05	1.08400E−04	2.57702E−05

Table 6 Statistical form of the LD model for $S_r(\tau)$ class

τ	$S_r(\tau)$					
	Min	Max	Med	SIR	SD	Mean
0	6.84986E−07	4.10222E−04	2.05132E−05	5.12879E−05	1.27031E−04	2.05132E−05
0.05	1.54202E−06	3.84817E−04	4.96561E−05	4.94712E−05	1.09446E−04	4.96561E−05
0.1	3.27210E−05	3.37500E−04	1.23714E−04	3.31713E−05	7.57222E−05	1.23714E−04
0.15	1.79588E−05	3.14947E−04	1.49635E−04	6.40012E−05	8.67490E−05	1.49635E−04
0.2	5.58908E−07	3.11098E−04	1.12951E−04	8.23980E−05	8.93637E−05	1.12951E−04
0.25	2.80288E−06	3.07499E−04	8.72434E−05	5.60759E−05	7.69075E−05	8.72434E−05
0.3	5.13924E−07	2.92941E−04	5.03546E−05	5.22810E−05	9.49974E−05	5.03546E−05
0.35	1.72647E−05	4.01126E−04	5.87674E−05	5.74047E−05	1.07739E−04	5.87674E−05
0.4	7.07416E−06	4.37458E−04	7.74465E−05	7.02966E−05	1.10540E−04	7.74465E−05
0.45	1.30053E−06	3.87521E−04	5.94169E−05	6.05638E−05	1.03835E−04	5.94169E−05
0.5	1.08795E−05	2.73571E−04	7.76476E−05	4.85662E−05	7.69163E−05	7.76476E−05
0.55	1.82368E−06	2.85865E−04	1.00356E−04	5.94903E−05	8.25418E−05	1.00356E−04
0.6	2.10866E−06	3.26146E−04	8.54391E−05	5.68847E−05	8.87066E−05	8.54391E−05
0.65	4.14752E−06	2.83154E−04	8.99094E−05	5.27638E−05	8.02371E−05	8.99094E−05
0.7	1.04316E−06	2.44741E−04	8.49671E−05	4.92785E−05	6.82708E−05	8.49671E−05
0.75	4.41183E−06	2.24144E−04	5.62133E−05	5.94390E−05	6.90455E−05	5.62133E−05
0.8	3.27763E−06	2.89477E−04	6.73767E−05	4.64627E−05	7.54554E−05	6.73767E−05
0.85	4.50773E−06	3.24620E−04	6.73931E−05	2.99961E−05	7.68969E−05	6.73931E−05
0.9	1.78758E−07	2.43798E−04	7.08003E−05	4.64861E−05	6.47135E−05	7.08003E−05
0.95	3.46180E−06	2.62461E−04	8.03727E−05	4.13648E−05	6.90339E−05	8.03727E−05
1	1.17841E−05	2.68730E−04	5.09659E−05	4.42562E−05	6.84191E−05	5.09659E−05

Table 7 Statistical form of the LD model for $I_r(\tau)$ class

τ	$I_r(\tau)$					
	Min	Max	Med	SIR	SD	Mean
0	1.39616E−06	1.37144E−04	2.04959E−05	2.43181E−05	4.18453E−05	2.04959E−05
0.05	4.68544E−07	2.16919E−04	2.98034E−05	3.50897E−05	5.57051E−05	2.98034E−05
0.1	1.08688E−06	1.47040E−04	3.68655E−05	3.47270E−05	3.87396E−05	3.68655E−05
0.15	1.10787E−05	1.48333E−04	3.30834E−05	1.80381E−05	3.68967E−05	3.30834E−05
0.2	1.55290E−06	1.78257E−04	4.97327E−05	4.19550E−05	5.22723E−05	4.97327E−05
0.25	4.24311E−06	2.37910E−04	5.73799E−05	6.09449E−05	6.85332E−05	5.73799E−05
0.3	1.32746E−05	3.04651E−04	6.12909E−05	6.10633E−05	7.75426E−05	6.12909E−05
0.35	2.78155E−06	3.26867E−04	5.77003E−05	4.57392E−05	7.89573E−05	5.77003E−05
0.4	1.89610E−06	3.04920E−04	4.62899E−05	4.05587E−05	7.08756E−05	4.62899E−05
0.45	1.47995E−06	2.46594E−04	3.53113E−05	3.27931E−05	5.87653E−05	3.53113E−05
0.5	4.94391E−07	1.64592E−04	3.20415E−05	3.26320E−05	4.96208E−05	3.20415E−05
0.55	7.40733E−06	1.87931E−04	4.29732E−05	2.61886E−05	4.32316E−05	4.29732E−05
0.6	2.32855E−06	2.17791E−04	3.96101E−05	3.40674E−05	5.22670E−05	3.96101E−05
0.65	7.25146E−06	2.36464E−04	4.44554E−05	3.92808E−05	6.16269E−05	4.44554E−05
0.7	1.03662E−05	2.41543E−04	3.39979E−05	3.18914E−05	7.40774E−05	3.39979E−05
0.75	4.12207E−06	2.74952E−04	3.71526E−05	4.18523E−05	8.29917E−05	3.71526E−05
0.8	3.43753E−07	2.77896E−04	5.82515E−05	3.68146E−05	8.43389E−05	5.82515E−05
0.85	1.62338E−06	2.63629E−04	7.06299E−05	5.58564E−05	7.87530E−05	7.06299E−05
0.9	3.10176E−06	2.77612E−04	7.04554E−05	5.90807E−05	7.81879E−05	7.04554E−05
0.95	3.12726E−06	2.52710E−04	6.55093E−05	7.85680E−05	8.46117E−05	6.55093E−05
1	4.37365E−06	2.50216E−04	6.57923E−05	6.95860E−05	8.12307E−05	6.57923E−05

Table 8 Global form of the LD nonlinear mathematical system

Class	G.MAD		G.TIC		G.EVAF	
	Mean	SIR	Mean	SIR	Mean	SIR
$\hat{S}_h(\tau)$	8.40860E−05	3.02527E−05	4.74289E−09	1.71221E−09	2.07525E−10	1.34071E−10
$\hat{I}_h(\tau)$	6.94187E−05	2.78370E−05	3.82365E−09	1.49744E−09	1.90625E−10	1.02471E−10
$\hat{R}_h(\tau)$	6.47481E−05	2.74182E−05	3.43381E−09	1.41145E−09	1.29261E−10	8.57088E−11
$S_r(\tau)$	6.47481E−05	2.74182E−05	4.46733E−09	2.24031E−08	2.12059E−10	1.21758E−10
$I_r(\tau)$	5.66103E−05	4.05683E−05	2.98859E−09	2.15977E−09	9.07505E−11	1.94878E−10

procedures based on the global search genetic algorithm and local search active-set algorithm scheme. Leptospirosis disease is considered one of the dangerous zoonotic diseases that is found worldwide with low/high level. It is through the rodents, which causes death among the people. The mathematical form of the Leptospirosis disease is based on the SIR model, and the solutions of the Leptospirosis disease-based SIR model have been presented using the ANNs-GA-ASA. The obtained performances of the numerical solutions of the Leptospirosis disease have been compared with the Runge–Kutta-based reference solutions. These performances have been overlapped with the matching of level 6–9, which indicate the correctness of the designed method. To authenticate the precision, exactness, reliability and competence of the stochastic ANNs-GA-ASA procedures, the statistical analysis has been presented with multiple runs for solving the Leptospirosis disease-based mathematical model. The reliability is obtained to observe each statistical operator for solving the Leptospirosis disease-based nonlinear mathematical model.

In future studies, the ANN-GA-ASA is capable to solve the fractional order models (Sabir et al. 2021b, 2020d, 2021c), fluid dynamic systems (Umar, et al. 2020; Sabir, et al. 2020) and singular systems of higher order (Sabir et al. 2020e; Sabir et al. 2020f).

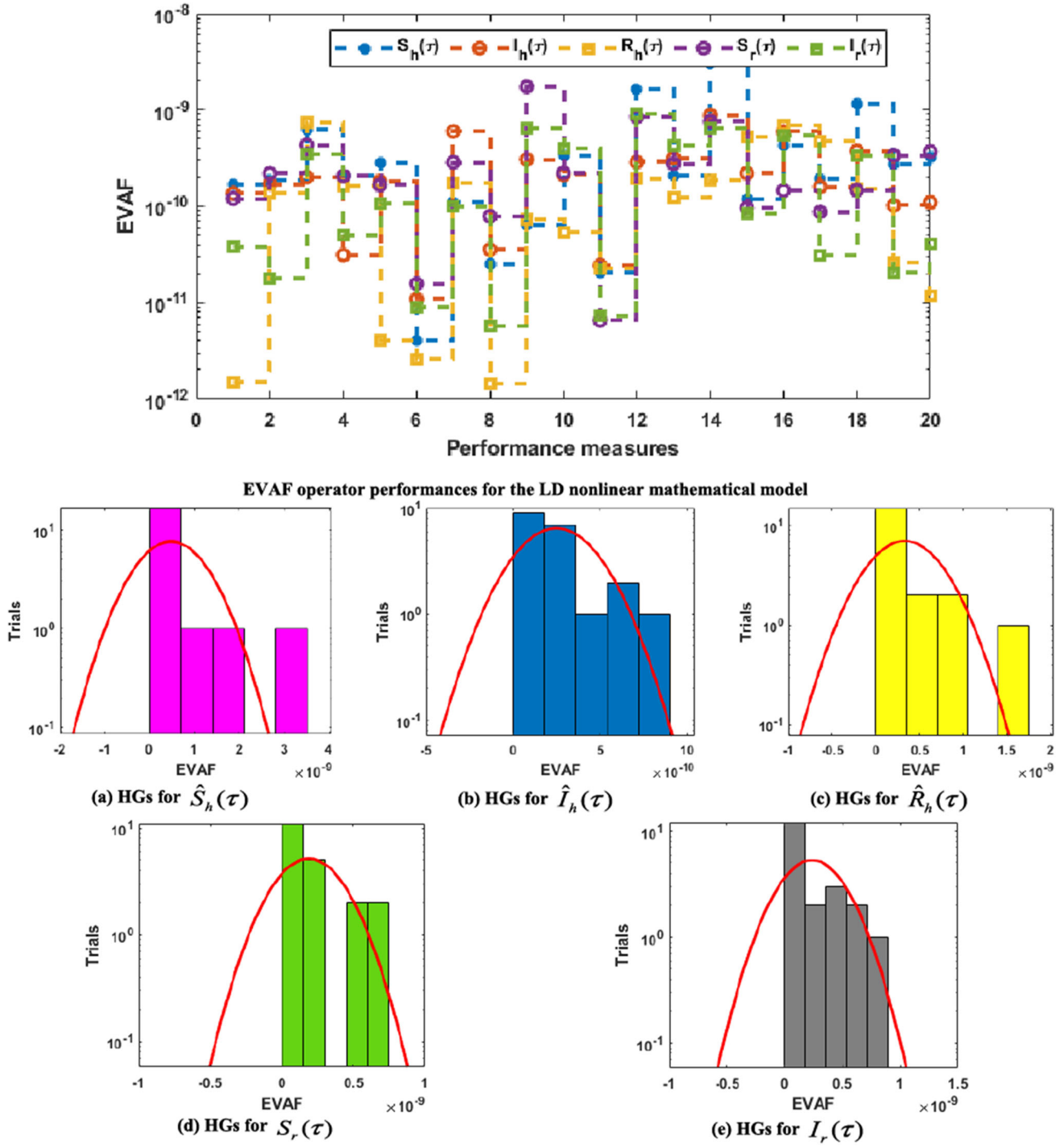

Fig. 8 EVAF convergence plots along with HGs using ANNs-GA-ASA to solve the LP model

Acknowledgements The first author was supported by the Program Management Unit for Human Resources & Institutional Development, Research and Innovation.

Data availability The datasets generated during and/or analyzed during the current study are available from the corresponding author on reasonable request.

Declarations

Conflict of Interest The authors declare that they have no conflict of interest.

References

Abide S, Barboteu M, Cherkaoui S, Dumont S (2021) A semi-smooth newton and primal-dual active set method for non-smooth contact dynamics. Comput Methods Appl Mech Eng 387:114153

Armaghani DJ, Hasanipanah M, Mahdiyar A, Majid MZA, Amnieh HB, Tahir MM (2018) Airblast prediction through a hybrid genetic algorithm-ANN model. Neural Comput Appl 29(9):619–629

Ayala HVH, dos Santos Coelho L (2012) Tuning of PID controller based on a multiobjective genetic algorithm applied to a robotic manipulator. Expert Syst Appl 39(10):8968–8974

Barboteu M, Dumont S (2018) A primal-dual active set method for solving multi-rigid-body dynamic contact problems. Math Mech Solids 23(3):489–503

Bhalraj A, Azmi A, Mohd MH (2021) Analytical and numerical solutions of leptospirosis model. Comput Sci 16(3):949–961

Bhalraj A and Azmi A (2019) Mathematical modelling of the spread of Leptospirosis. In: AIP Conference Proceedings (Vol. 2184, No. 1, p. 060031). AIP Publishing LLC

de Paiva JL, Toledo CF, Pedrini H (2016) An approach based on hybrid genetic algorithm applied to image denoising problem. Appl Soft Comput 46:778–791

Deuerlein JW, Piller O, Elhay S, Simpson AR (2019) Content-based active-set method for the pressure-dependent model of water distribution systems. J Water Resour Plan Manag 145(1):04018082

El-Shahed M (2014) Fractional order model for the spread of leptospirosis. Int J Math Anal 8(54):2651–2667

Gero MBP, García AB, del Coz Díaz JJ (2005) A modified elitist genetic algorithm applied to the design optimization of complex steel structures. J Constr Steel Res 61(2):265–280

Goh SH, Ismail R, Lau SF, Megat Abdul Rani PA, Mohd Mohidin TB, Daud F, Bahaman AR, Khairani-Bejo S, Radzi R, Khor KH (2019) Risk factors and prediction of leptospiral seropositivity among dogs and dog handlers in Malaysia. Int J Environ Res Public Health 16(9):1499

Guerrero Sánchez Y, Sabir Z, Günerhan H and Baskonus HM (2020) Analytical and approximate solutions of a novel nervous stomach mathematical model. Discret Dyn Nat Soc 2020.

Guirao JL et al. (2020) Design and numerical solutions of a novel third-order nonlinear emden–fowler delay differential model. Math Probl Eng 2020

Hassoon M, Kouhi MS, Zomorodi-Moghadam M and Abdar M (2017). Rule optimization of boosted c5. 0 classification using genetic algorithm for liver disease prediction. In 2017 international conference on computer and applications (icca) (pp. 299–305). IEEE.

He X and Yang P (2019) The primal-dual active set method for a class of nonlinear problems with-monotone operators. Math Prob Eng 2019

Keeling M (2001) The mathematics of diseases. Plus Mag 14

Keeling MJ, Rohani P (2011) Modeling infectious diseases in humans and animals. Princeton University Press

Khan MA, Saddiq SF, Islam S, Khan I, Shafie S (2016) Dynamic behavior of leptospirosis disease with saturated incidence rate. Int J Appl Comput Math 2(4):435–452

Khan MF, Alrabaiah H, Ullah S, Khan MA, Farooq M, Bin Mamat M, Asjad MI (2021) A new fractional model for vector-host disease with saturated treatment function via singular and non-singular operators. Alex Eng J 60(1):629–645

Kongnuy R (2012) Local stability of equilibria: leptospirosis. Int J Math Comput Sci 6(6):625–629

Lee ZJ and Lee WL (2003) A hybrid search algorithm of ant colony optimization and genetic algorithm applied to weapon-target assignment problems. In: International Conference on Intelligent Data Engineering and Automated Learning (pp. 278–285). Springer, Berlin, Heidelberg.

Lim JK, Murugaiyah VA, Ramli AS, Rahman HA, Mohamed NSF, Shamsudin NN and Tan JC (2011) A case study: leptospirosis in Malaysia

Motieghader H, Najafi A, Sadeghi B, Masoudi-Nejad A (2017) A hybrid gene selection algorithm for microarray cancer classification using genetic algorithm and learning automata. Inform Med Unlocked 9:246–254

Oliveira AL, Braga PL, Lima RM, Cornélio ML (2010) GA-based method for feature selection and parameters optimization for machine learning regression applied to software effort estimation. Inform Softw Technol 52(11):1155–1166

Oyama A, Obayashi S, Nakamura T (2001) Real-coded adaptive range genetic algorithm applied to transonic wing optimization. Appl Soft Comput 1(3):179–187

Pereira CM, Lapa CM (2003) Coarse-grained parallel genetic algorithm applied to a nuclear reactor core design optimization problem. Ann Nucl Energy 30(5):555–565

Quirynen R, Knyazev A, Di Cairano S, (2018) Block structured preconditioning within an active-set method for real-time optimal control. In 2018 European Control Conference (ECC) (pp. 1154–1159). IEEE.

Raja MAZ et al (2018) A new stochastic computing paradigm for the dynamics of nonlinear singular heat conduction model of the human head. Eur Phys J Plus 133(9):364

Sabir Z et al (2018) Neuro-heuristics for nonlinear singular Thomas–Fermi systems. Appl Soft Comput 65:152–169

Sabir Z et al (2020a) Neuro-swarm intelligent computing to solve the second-order singular functional differential model. Eur Phys J Plus 135(6):474

Sabir Z et al (2020b) A neuro-swarming intelligence based computing for second order singular periodic nonlinear boundary value problems. Front Phys 8:224. https://doi.org/10.3389/fphy.2020.00224

Sabir Z et al (2020c) FMNEICS: fractional Meyer neuro-evolution-based intelligent computing solver for doubly singular multi-fractional order Lane–Emden system. Comput Appl Math 39(4):1–18

Sabir Z, Raja MAZ, Shoaib M, Aguilar JG (2020d) FMNEICS: fractional Meyer neuro-evolution-based intelligent computing solver for doubly singular multi-fractional order Lane–Emden system. Comput Appl Math 39(4):1–18

Sabir Z et al (2020e) Integrated intelligent computing with neuro-swarming solver for multi-singular fourth-order nonlinear Emden–Fowler equation. Comput Appl Math 39(4):1–18

Sabir Z et al (2020f) Numerical investigations to design a novel model based on the fifth order system of Emden–Fowler equations. Theor Appl Mech Lett 10(5):333–342

Sabir Z, Raja MAZ, Baleanu D (2021b) Fractional Mayer Neuro-swarm heuristic solver for multi-fractional order doubly singular model based on Lane–Emden equation. Fractals 29(5):2140017–2141219

Sabir Z, Raja MAZ, Guirao JL, Shoaib M (2021c) A novel design of fractional meyer wavelet neural networks with application to the nonlinear singular fractional Lane–Emden systems. Alex Eng J 60(2):2641–2659

Sabir Z et al. (2020) Design of stochastic numerical solver for the solution of singular three-point second-order boundary value problems. Neural Comput Appl 1–17

Sabir Z, Umar M, Raja MAZ and Baleanu D (2021a) Applications of Gudermannian neural network for solving the SITR fractal system. Fractals.

Sabir Z, et al. (2020) The effects of activation energy and thermophoretic diffusion of nanoparticles on steady micropolar fluid along with Brownian motion. Adv Mater Sci Eng 2020.

Sánchez YG, Sabir Z, Guirao JL (2020) Design of a nonlinear SITR fractal model based on the dynamics of a novel coronavirus (COVID-19). Fractals 28(08):2040026

Shl GUOYONG (1997) A genetic algorithm applied to a classic job-shop scheduling problem. Int J Syst Sci 28(1):25–32

Song H, Wang X, Zhang K, Zhang Q (2017) Primal-dual active set method for American lookback put option pricing. East Asian J Appl Math 7(3):603–614

Thayaparan S, Robertson ID, Fairuz A, Suut L, Abdullah MT (2013) Leptospirosis, an emerging zoonotic disease in Malaysia. Malays J Pathol 35(2):123–132

Toledo CFM, De Oliveira RRR, França PM (2013) A hybrid multi-population genetic algorithm applied to solve the multi-level capacitated lot sizing problem with backlogging. Comput Oper Res 40(4):910–919

Triampo W, Baowan D, Tang IM, Nuttavut N, Wong-Ekkabut J, Doungchawee G (2007) A simple deterministic model for the spread of leptospirosis in Thailand. Int J Bio Med Sci 2:22–26

Umar M et al (2019a) Unsupervised constrained neural network modeling of boundary value corneal model for eye surgery. Appl Soft Comput 85:105826

Umar M et al (2019b) Intelligent computing for numerical treatment of nonlinear prey–predator models. Appl Soft Comput 80:506–524

Umar M et al (2020) The 3-D flow of Casson nanofluid over a stretched sheet with chemical reactions, velocity slip, thermal radiation and Brownian motion. Therm Sci 24(5):2929–2939

Umar M, Sabir Z, Raja MAZ, Sánchez YG (2020a) A stochastic numerical computing heuristic of SIR nonlinear model based on dengue fever. Results Phys 19:103585

Umar M et al (2020b) Stochastic numerical technique for solving HIV infection model of CD4+T cells. Eur Phys J Plus 135(6):403

Umar M et al (2020c) A stochastic computational intelligent solver for numerical treatment of mosquito dispersal model in a heterogeneous environment. Eur Phys J Plus 135(7):1–23